Efficient Sensor Location for HVAC Systems Using Lagrangian Coherent Structures

Hindawi
Mathematical Problems in Engineering
Volume 2023, Article ID 6059900, 13 pages
https://doi.org/10.1155/2023/6059900

Research Article

Efficient Sensor Location for HVAC Systems Using Lagrangian Coherent Structures

Dildar Ahmed,[1] **Ali Javed**,[2] **M. Sami Uz Zaman**,[1] **Minhas Mahsud**,[1] **and Mumuni-Napari Hanifatu**[3]

[1]*National University of Sciences and Technology, Islamabad, Pakistan*
[2]*Pakistan Institute of Engineering and Applied Sciences, Islamabad, Pakistan*
[3]*Tamale Technical University, Tamale, Ghana*

Correspondence should be addressed to Mumuni-Napari Hanifatu; hmnapari@tatu.edu.gh

Received 3 September 2022; Revised 1 December 2022; Accepted 18 April 2023; Published 13 June 2023

Academic Editor: Amr Elsonbaty

Study of thermo-fluid flow has its significance in energy analysis of a building. Various thermo-fluid analyses are performed in heating ventilation and air conditioning (HVAC) systems for energy efficient buildings by scientists and engineers to save energy consumption during the life of a building. In order to achieve energy conservation for different HVAC systems, determination of air flow pattern and flow physics are vital parameters. In case of fluid flow postprocessing techniques such as streamlines, vector plots and contours are often employed. These techniques help in understanding the nature of flow and its properties. Each of these postprocessing techniques mentioned are based on Eulerian methods and have certain inherent deficiencies pertaining to the amount of information they can convey about certain aspects of fluid flow. Lagrangian coherent structures (LCS) on the other hand use Lagrangian data for analysis purposes. LCS are generated using finite time Lyapunov exponent fields which in turn depict the rate of expansion or contraction of the trajectories around a certain point. LCS act as the transport barriers across which there is approximately zero mass flux. This property means that LCS can be applied to problems related to separation and reattachment in fluid flow and find virtual boundaries inside flows. In the current study, we focused on the application of LCS for efficient placement of sensors for HVAC systems. We computed LCS using velocity data extracted from the CFD simulations of a 2D room model. Thus, LCS can be used to identify the virtual boundaries in fluid flow. This helps in indication of regions where mixing of particles occurs and also where particles are stagnated. Inlet angles of 0, 15, 22, and 30 degrees are used and analysis shows that manifolds with 30 degree angles provide better ventilation. The outcome of this study can be used to improve the energy efficiency as well as predict the accurate location of HVAC sensor and control units.

1. Introduction

The building stock includes residential, commercial, institutional, and public structures. Energy efficiency means utilizing the minimum amount of energy for heating, cooling, equipment, and lighting that is required to maintain comfort conditions in a building. An important factor impacting on energy efficiency is the building envelope. This includes all of the building elements between the interior and the exterior of the building such as walls, windows, doors, roof, and foundations. All of these components must work together in order to keep the building cool in the summer and warm in the winter [1, 2]. The amount of energy consumed varies depending on the design of the fabric of the building and its systems and how they are operated. The heating and cooling systems consume the most energy in a building; however, controls such as programmable thermostats and building energy management systems can significantly reduce the energy use of these systems. Some buildings also use zone heating and cooling systems, which can reduce heating and cooling in the unused areas of a building. In commercial buildings, integrated space and water heating systems can provide the best approach to energy efficient heating [3]. Commercial buildings include

a wide variety of building types such as offices, hospitals, schools, police stations, places of worship, warehouses, hotels, libraries, and shopping malls. These different commercial activities all have unique energy needs but, as a whole, commercial buildings use more than half their energy for heating and lighting [4]. In commercial buildings the most common fuel types used are electricity and natural gas. Occasionally, commercial buildings also utilize another source of energy in the form of locally generated group or district energy in the form of heat and/or power.

There are two perspectives while studying the fluid flow behavior; one is Eulerian and other is Lagrangian. In Eulerian approach, properties of flow field are observed in a fixed space and time irrespective of identity of fluid particles. On the other hand, in Lagrangian perspective, the identity of individual fluid elements is concerned. The changing velocity of the particles is tracked along their paths as they are adverted by the flow. Lagrangian coherent structures method is used to identify dynamic manifolds in fluid flows. A Lagrangian coherent structure is a mobile separatrix with zero mass flux property or with minimum leak. LCS is a material line that is defined as the smooth curves of fluid particles that acts as a transport barrier and is an invariant manifold. These structures are called Lagrangian because they use a series of time steps defining the motion of fluid particles to calculate instead of the Eulerian approach, that only uses instantaneous time frames. The term coherent structure in the name is used because the LCS delineates the familiar coherent structures associated with the flow. LCS method uses material lines that have locally maximum attraction or repulsion to the fluid particles. The definition of coherent structures has been vague in the past, despite their importance. This has made it difficult to properly identify and extract them. Hyperbolic structures have been studied widely in past in periodic and steady systems [5, 6]. The study of stable and unstable manifolds in such systems is simpler then unsteady and aperiodic time.

George Haller was the first researcher to provide a general definition to Lagrangian coherent structures for time dependent systems [7, 8]. Haller used a finite time interval in his approach to define LCS. He was also the first to introduce hyperbolic time approach in his seminal papers. Lagrangian coherent structures were defined as the ridges of finite time Lyapunov exponent fields by Shadden et al. [9]. In the past, Lagrangian coherent structures have been used in several real life applications. Usage of Lagrangian coherent structures to analyze the pollution release of the coast of Florida has been performed in the past [10]. The problem was associated with knowing the exact time and location for pollution release so that it drifted away into the ocean instead of returning to the shore. As LCS structures are the virtual boundaries in the fluid, it was possible to identify the locations of LCS and determine on which locations and times are suitable for pollutant release. Similarly, wake formation for flow over a cylinder [11] and structure of aortic valve jet [12] and flow control over an airfoil is there as well. Assorted works of Shadden [13] were the applications of Lagrangian coherent structures. The literature review in the form of a table is presented herewith for better understanding. Table 1 presents the summary of the literature review.

2. Methodology

2.1. Air Flow Analysis in a 2D Room Model. To study the air flow pattern, a 2D room model was used. The length and height of the room are 9 meters and 3 meters, respectively. An inlet slot is made in the top left near the wall having a height of 0.168 meters and outlet slot is made in the bottom right near the wall having a height of 0.48 meters as shown in Figure 1. Air is introduced from the inlet with inlet velocity 0.455 m/s. The Reynolds number is 5000, based on inlet air velocity, inlet width, and properties of air, which creates turbulent flow and introduces circulation into the cavity. We computed horizontal and vertical components of velocity along vertical lines at $x = 3$ m and $x = 6$ m and along horizontal lines at $y = 0.084$ m and $y = 2.916$ m as shown in Figure 2. Results from the calculations are presented with the result of Kayne and Agarwal [14].

For the conservation of mass and momentum of fluid flow, continuity and momentum equation are used as follows.

2.1.1. Continuity Equation. The continuity equation is given by the following equation:

$$\frac{\partial \rho}{\partial t} + \frac{\partial (\rho u_i)}{\partial x_i} = 0. \tag{1}$$

2.1.2. Momentum Equation. The momentum equation is given bythe following equation:

$$\frac{\partial (\rho u_i)}{\partial t} + \frac{\partial \left(\rho u_j u_i\right)}{\partial x_j} = -\frac{-\partial p}{\partial x_i} + \mu \frac{\partial^2 u_i}{\partial x_j \partial x_j}, \tag{2}$$

where $i, j = 1, 2$; u_i represents the Cartesian velocity components (u, v); ρ is fluid density; p is pressure; and μ is fluid dynamic or absolute viscosity.

To numerically simulate turbulent flow, we used standard k-ε Model. It is a two-equation model based on model transport equations for the turbulence kinetic energy (k) and its dissipation rate (ε). Transport equation for turbulence kinetic energy (k) and its dissipation rate (ε) are as follows:

Table 1: Summary of the literature review.

Author	Year	Salient
Kedar	1990	Examine the transport properties of a particular 2D incompressible flow using dynamical systems techniques
Haller	2000	Derived analytical criterion to extract coherent structures and applied it to 2D barotropic turbulence simulation
Haller	2002	Examines whether hyperbolic Lagrangian structures found in model velocity data represent reliable predictions for mixing in the true fluid velocity field
Shadden	2005	Developed theory of Lagrangian coherent structures applicable to flows over finite interval of time
Tian	2006	Ventilated model room to evaluate turbulence prediction in indoor airflow
Evola	2006	CFD models for wind driven natural ventilation in a cubic building
Stankov	2006	Numerically modeled office room for thermal comfort of occupants
Kayne	2013	CFD computations using RANS equation in 3D building enclosure
Kermani	2015	Investigate ventilation in a hospital room
Alhashme	2016	Cases with different inlet velocity, heating, and cooling systems were tested
Olcay	2016	Flow over a cylinder using CFD and finite time Lyapunov exponent fields

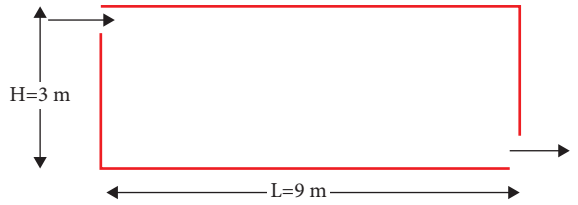

Figure 1: Sketch of the 2D model for airflow.

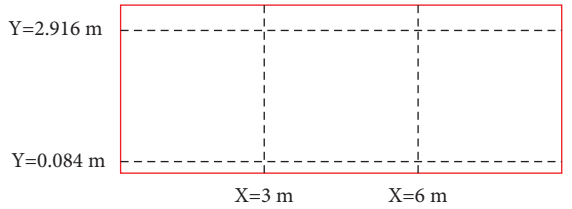

Figure 2: Partition lines for observation of U and V components of velocity.

$$\frac{\partial(\rho k)}{\partial t}+\frac{\partial(\rho k u_i)}{\partial x_i}=\frac{\partial}{\partial x_j}\left[\left(\mu+\frac{\mu_t}{\sigma_k}\right)\frac{\partial k}{\partial x_j}\right]+G_k+G_b-\rho\varepsilon-Y_M+S_k,$$

$$\frac{\partial(\rho\varepsilon)}{\partial t}+\frac{\partial(\rho\varepsilon u_i)}{\partial x_i}=\frac{\partial}{\partial x_j}\left[\left(\mu+\frac{\mu_t}{\sigma_\varepsilon}\right)\frac{\partial\varepsilon}{\partial x_j}\right]+C_{1\varepsilon}\frac{\varepsilon}{k}\left(G_k+C_{3\varepsilon}G_b\right)-C_{2\varepsilon}\rho\frac{\varepsilon^2}{k}+S_\varepsilon. \tag{3}$$

The left side of both equations represents the rate of change of k or ε and transport of k or ε by convection, while the right side of both equations represents transport of k or ε by diffusion, rate of production of k or ε, and rate of destruction of k or ε.

The turbulent (or eddy) viscosity (μ_t) is computed by combining k and ε as follows:

$$\mu_t=\rho C_\mu\frac{k^2}{\varepsilon}. \tag{4}$$

The values of constants used in the above equations are as follows:

$$\begin{aligned} C_{1\varepsilon} &= 1.44, \\ C_{2\varepsilon} &= 1.92, \\ C_{\mu} &= 0.09, \\ \sigma_k &= 1.0, \\ \sigma_{\varepsilon} &= 1.3. \end{aligned} \tag{5}$$

The driving force for fluid flow in momentum equation is pressure term, but there is no transport equation for the case of incompressible flow. Due to nonlinearity and coupling between pressure and velocity, iterative guess and correct method would be required. In the current study, semi-implicit method for pressure linked equations (SIMPLE) is used to couple pressure and velocity. To solve the momentum, turbulent kinetic, and dissipation rate, second-order upwind scheme is used. The second-order upwind scheme uses a Taylor expansion of the upstream cell about the cell centered data. The least squares cell based (LSCB) and second order spatial discretization are used for the gradient and pressure, respectively. First-order implicit method is used for temporal discretization. Let us now move towards the results section.

3. Results

The horizontal component of the velocity in nondimensional form along vertical lines at $x = 3$ m and $x = 6$ m is presented in Figure 3.

The horizontal component of velocity in nondimensional form also computed along horizontal lines at $y = 0.084$ m and $y = 2.916$ m is shown in Figure 4.

The vertical component of velocity in nondimensional form along vertical lines at $x = 3$ m and $x = 6$ m is presented in Figure 5. The velocity profiles at these lines are parabolic in nature. The velocity profile along a vertical line at $x = 6$ m is inverse parabola as compared to velocity profile along a vertical line at $x = 3$ m, which shows recirculation of air in 2D cavity.

3.1. Model Verification. In order to verify the above mentioned results, we computed these results at three different grid/mesh sizes. The number of mesh elements is 0.04 million, 0.05 million, and 0.06 million. The belowmentioned results in Figures 6(a)–6(d) show mesh independency achieved and the results do not change in a significant manner as further refinement of mesh elements.

3.2. Model Validation. For model validation, we compared our results with the results of Kayne and Agarwal [14]. In this validation, we also computed L_2 relative error norm, which is 0.08 for the horizontal component of velocity along a vertical line at $x = 3$ m and 0.10 for the horizontal component of velocity along a vertical line at $x = 6$ m. The results shown in Figures 7(a) and 7(b).

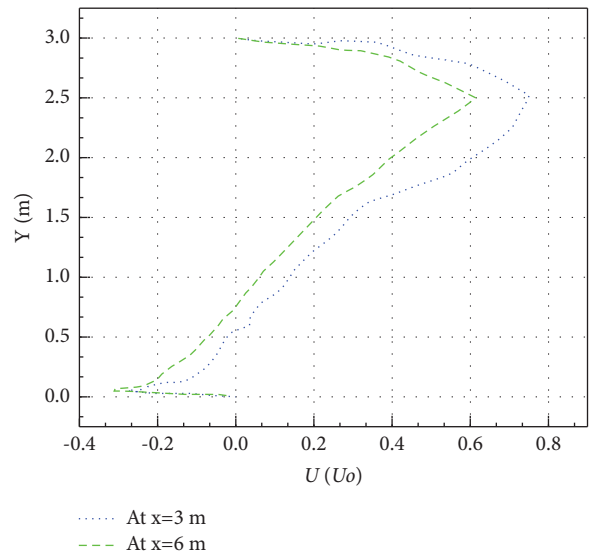

Figure 3: U/U_o velocity along $x = 3$ m and $x = 6$ m.

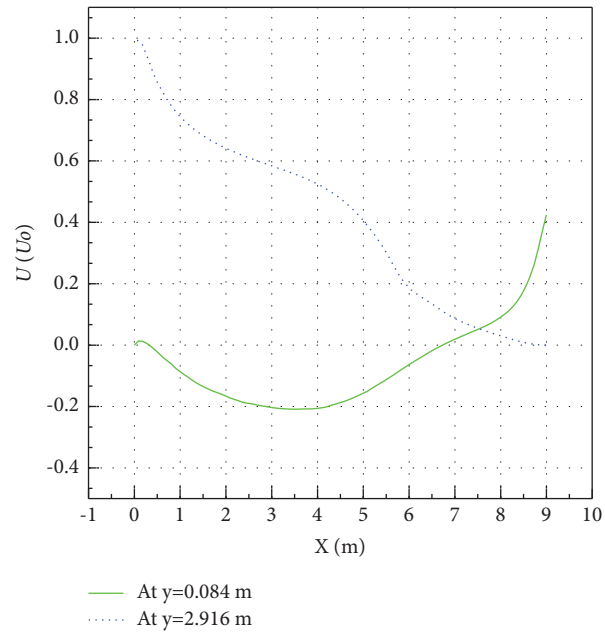

Figure 4: U/U_o velocity along $y = 0.084$ m and $y = 2.916$ m.

The computational fluid dynamics (CFD) postprocessing results are presented in the form of velocity contours and vector plot. Figures 8(a)–8(c) represent the horizontal velocity contour u, vertical velocity contour v, and velocity vectors, respectively, in 2D model room.

3.3. Lagrangian Coherent Structures (LCS). In the study of dynamical systems a separatrix can be defined as a manifold attached to fixed points across which there is zero mass flux. In case of fluid flow and many such physical problems, the fixed points are not stationary. In fact, they can be constantly moving with time. This presents a problem in using traditionally analytical techniques for dynamical systems to find

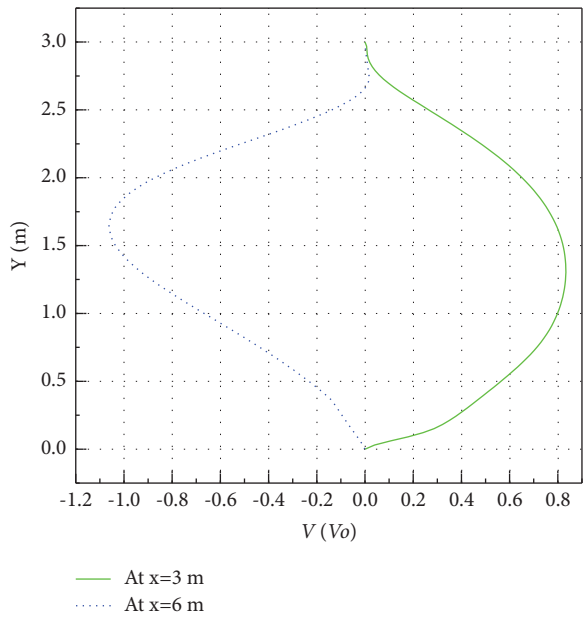

FIGURE 5: V/V_o velocity along $x = 3$ m and $x = 6$ m.

these manifolds in fluid flow. To tackle this problem a technique of Lagrangian coherent structures is used to identify these dynamic manifolds in fluid flows. Lagrangian coherent structure is a mobile separatrix with zero mass flux property or with minimum leak. LCS is a material line that is defined as the smooth curves of fluid particles that acts as a transport barrier and is an invariant manifold. These structures are called Lagrangian because they use a series of time steps defining the motion of fluid particles to calculate instead of the Eulerian approach, that only uses instantaneous time frames [11, 15]. The term coherent structures in the name are used because the LCS delineates the familiar coherent structures associated with the flow. LCS use material lines that have locally maximum attraction or repulsion to the fluid particles. The property that LCS use material lines with maximum local attraction and repulsion can be used to compute them. This technique uses finite time Lyapunov exponents (FTLE). A domain or particles is integrated in time to find the trajectories of particles after a certain finite time. This information is then used to calculate the FTLE field [16]. The rides in the FTLE field depict the manifolds or material lines. For the computation of repelling material lines or stable manifolds, the particles are integrated forward in time, while for the computation of unstable manifolds or attracting material lines, particles are integrated backwards in time as the expansion of particles in backward time simulation will represent the attraction of particles in forward time simulation.

3.3.1. Finite Time Lyapunov Exponents (FTLE). The classical Lyapunov exponent $\lim_{T \longrightarrow \infty} \sigma_{t_0}^{T}$ is useful in the study of Ergodic theory for time independent dynamical systems. It measures the rates of expansion and contraction of trajectories surrounding it. Lyapunov exponents are asymptotic quantities and describe the rate at which a perturbation to a trajectory grows or decays at a certain location in time. However, many dynamical systems especially fluid flow applications are time dependent and only computed or measured over a finite interval of time. Because of its asymptotic nature, the classical Lyapunov exponent is not suited for analyzing time dependent dynamical systems or those that are only defined on a finite time interval, so its value is quite limited for practical analyses. Nonetheless, the finite time Lyapunov exponent is applicable to many time dependent applications that are defined by a discrete set of data points. The finite time Lyapunov exponent (FTLE), denoted by $\sigma_t^T(x)$, is a scalar value which characterizes the amount of stretching about the trajectory of point $x \in D$ over the time interval (t, $t + T$). For most flows of practical importance, the FTLE varies as a function of space and time. The FTLE is not an instantaneous separation rate rather it measures the average or integrated separation between trajectories. This distinction is important because in time dependent flows, the instantaneous velocity field often is not very revealing about actual trajectories, that is, instantaneous streamlines can quickly diverge from actual particle trajectories. However, the FTLE accounts for the integrated effect of the flow because it is derived from the particle trajectories, and thus is more indicative of the actual transport behavior.

Consider an arbitrary point $x \in D$ at time t_0 which is advected by the flow after a time interval T. The flow has a continuous dependence on initial conditions and an arbitrary point near x at time t_0 will behave similarly as x when adverted in the flow, at least locally in time. However, as time evolves, the distance between this neighboring point and the point x will almost certainly change. Consider the evolution of a point close to x, which is written as $y = x + \delta x(t_0)$, where $\delta x(t_0)$ is infinitesimal and arbitrarily oriented. After time interval T, this perturbation becomes

$$\begin{aligned} \mathbf{x} &\longmapsto \varnothing_{t_0}^{t_0+T}(\mathbf{x}), \\ \delta\mathbf{x}(t_0+T) &= \varnothing_{t_0}^{t_0+T}(\mathbf{y}) - \varnothing_{t_0}^{t_0+T}(\mathbf{x}) \\ &= \frac{d\varnothing_{t_0}^{t_0+T}(\mathbf{x})}{d\mathbf{x}}\delta\mathbf{x}(t_0) + \mathrm{O}\left(\left\|\delta\mathbf{x}(t_0)\right\|^2\right). \end{aligned} \tag{6}$$

The second equality comes from taking the Taylor series expansion of the flow about point $\mathbf{x}$. Since $\delta x(t_0)$ is infinitesimal, therefore, $\mathrm{O}(\|\delta\mathbf{x}(t_0)\|^2)$ term is negligible. The magnitude of perturbation using standard vector L_2-norm is given by the following equation:

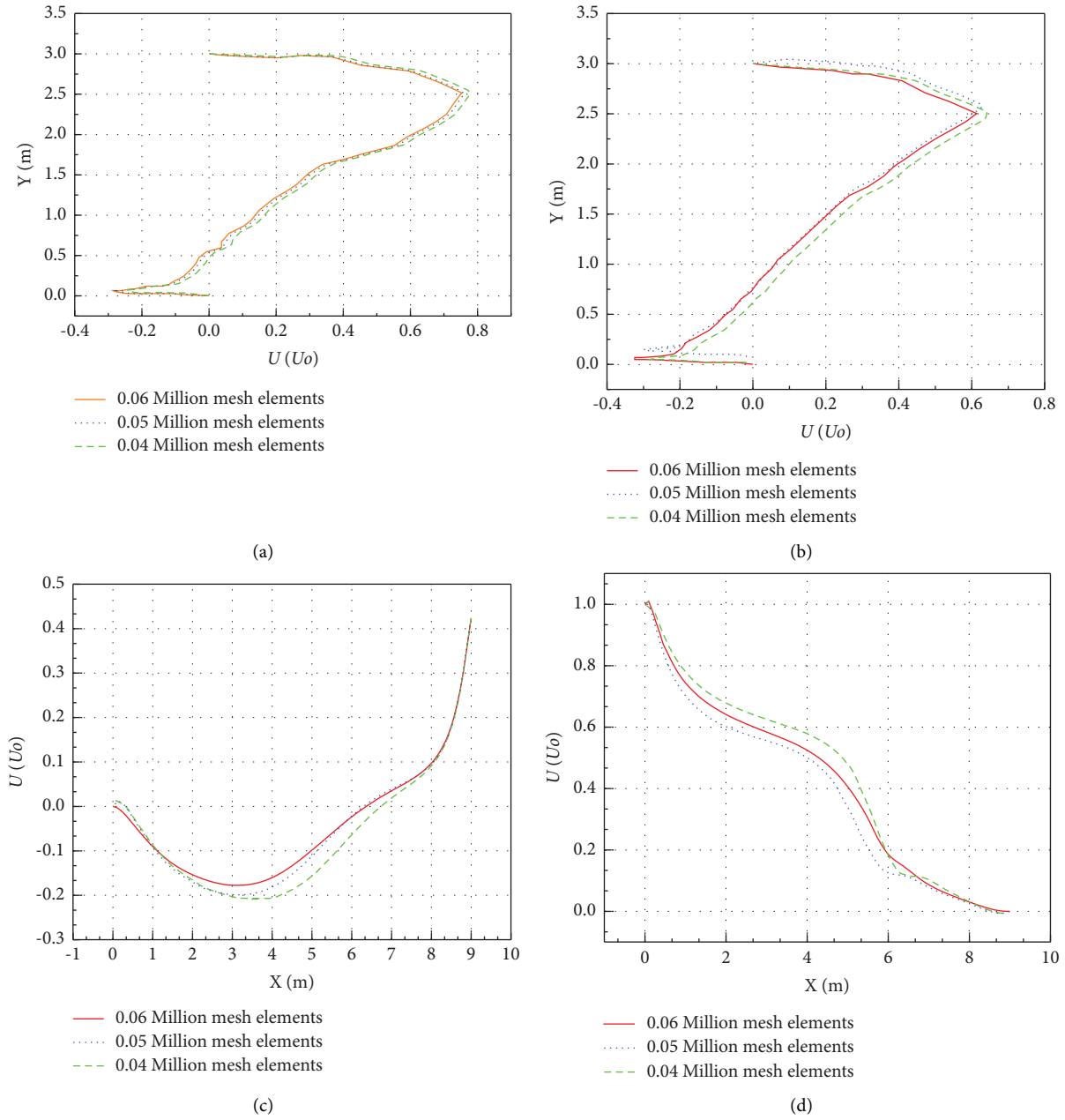

Figure 6: (a) Comparison of present CFD results with three different number of mesh elements at $x = 3$ m. (b) Comparison of present CFD results with three different number of mesh elements at $x = 6$ m. (c) Comparison of present CFD results with three different number of mesh elements at $y = 0.084$ m. (d) Comparison of present CFD results with three different number of mesh elements at $y = 2.916$ m.

$$\left\|\delta\mathbf{x}(t_0+T)\right\| = \sqrt{\left\langle \frac{d\varnothing_{t_0}^{t_0+T}(\mathbf{x})}{d\mathbf{x}}\delta\mathbf{x}(t_0), \frac{d\varnothing_{t_0}^{t_0+T}(\mathbf{x})}{d\mathbf{x}}\delta\mathbf{x}(t_0)\right\rangle} = \sqrt{\left\langle \delta\mathbf{x}(t_0), \frac{d\varnothing_{t_0}^{t_0+T}(\mathbf{x})}{d\mathbf{x}}\cdot\frac{d\varnothing_{t_0}^{t_0+T}(\mathbf{x})}{d\mathbf{x}}\delta\mathbf{x}(t_0)\right\rangle}. \tag{7}$$

We can write

$$\Delta = \frac{d\varnothing_{t_0}^{t_0+T}(\mathbf{x})}{d\mathbf{x}}\cdot\frac{d\varnothing_{t_0}^{t_0+T}(\mathbf{x})}{d\mathbf{x}}\delta\mathbf{x}(t_0), \tag{8}$$

where Δ is a symmetric matrix. To find out the maximum stretching between two points x and y, we are interested in the value of $\delta x(t_0)$ that is aligned with the eigenvector that gives the highest eigenvalue of Δ. Hence, an expression can be written as follows:

$$\begin{aligned}\max_{\delta\mathbf{x}(t_0)}\left\|\delta\mathbf{x}(t_0+T)\right\| &= \sqrt{\left\langle\overline{\delta\mathbf{x}}(t_0), \boldsymbol{\lambda}_{\max}(\Delta)\overline{\delta\mathbf{x}}(t_0)\right\rangle} \\ &= \sqrt{\boldsymbol{\lambda}_{\max}(\Delta)}\left\|\overline{\delta\mathbf{x}}(t_0)\right\|,\end{aligned} \tag{9}$$

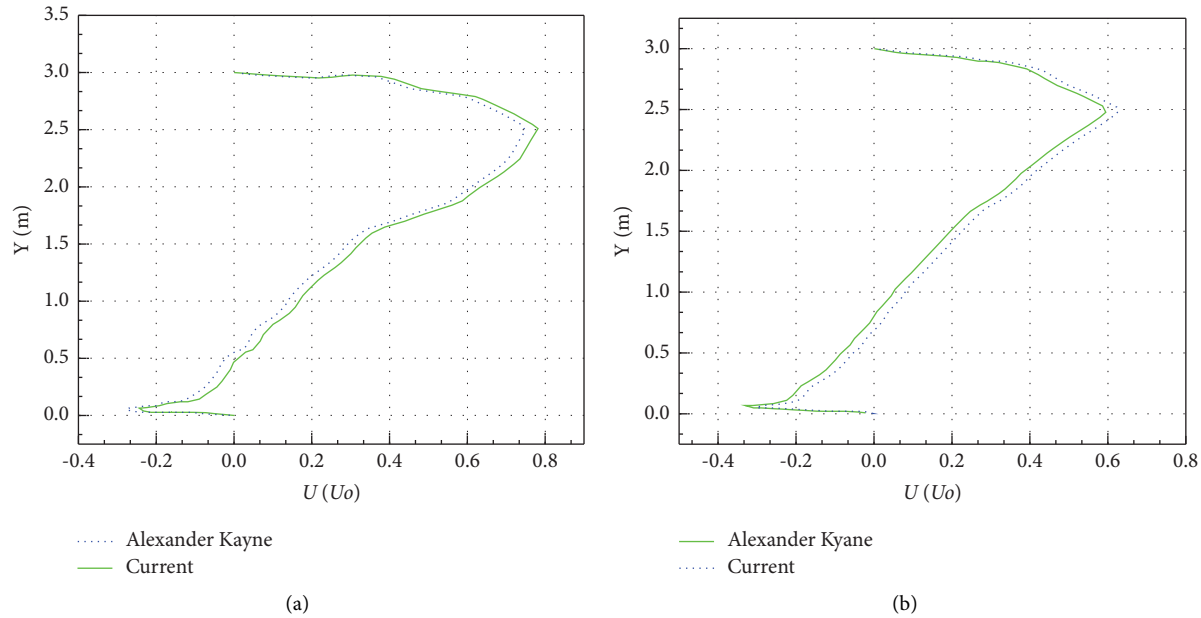

Figure 7: (a) Comparison of present CFD result with the computations of Kayne and Agarwal [14] at $x = 3$ m. (b) Comparison of present CFD result with the computations of Kayne and Agarwal [14] at $x = 6$ m.

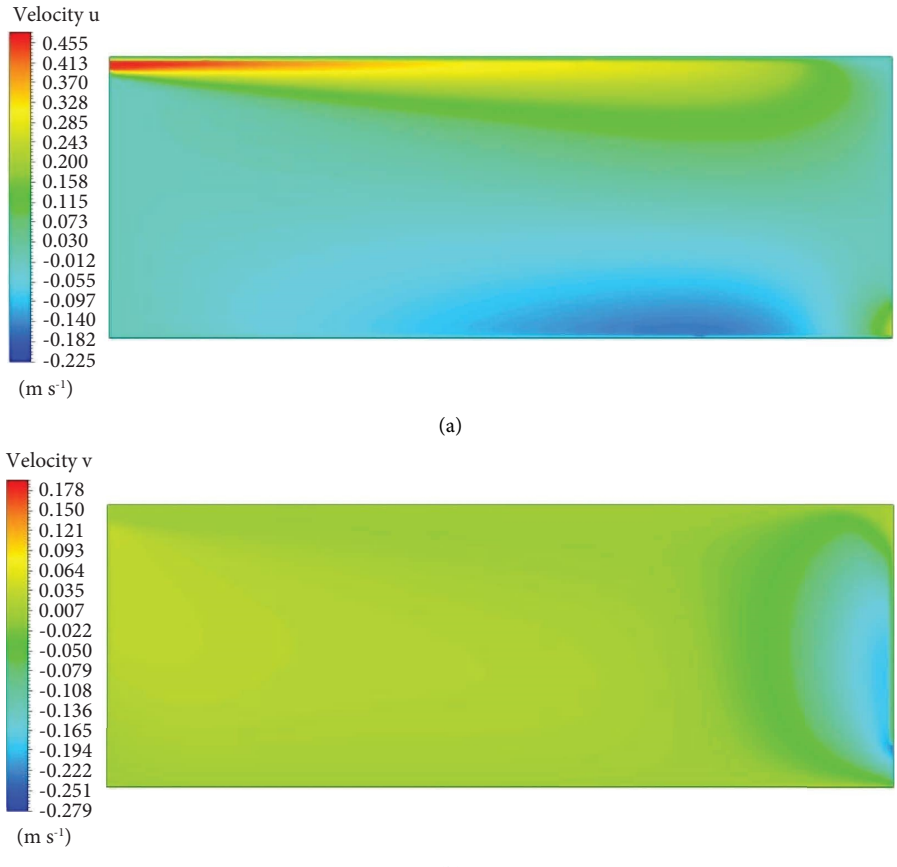

Figure 8: Continued.

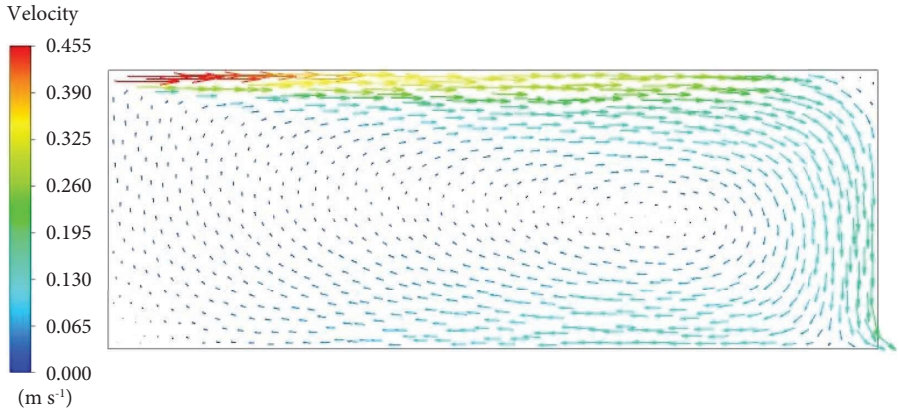

(c)

Figure 8: (a) u velocity contours in 2D model room. (b) v velocity contours in 2D model room. (c) Velocity vectors in 2D model room.

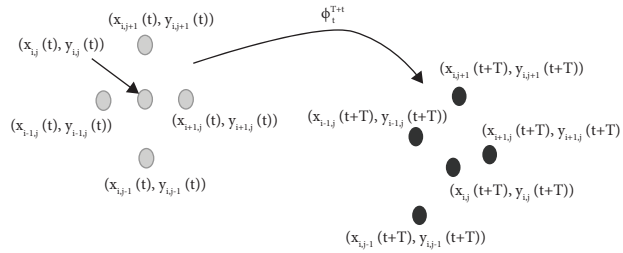

Figure 9: Particles in domain at time $t + T$.

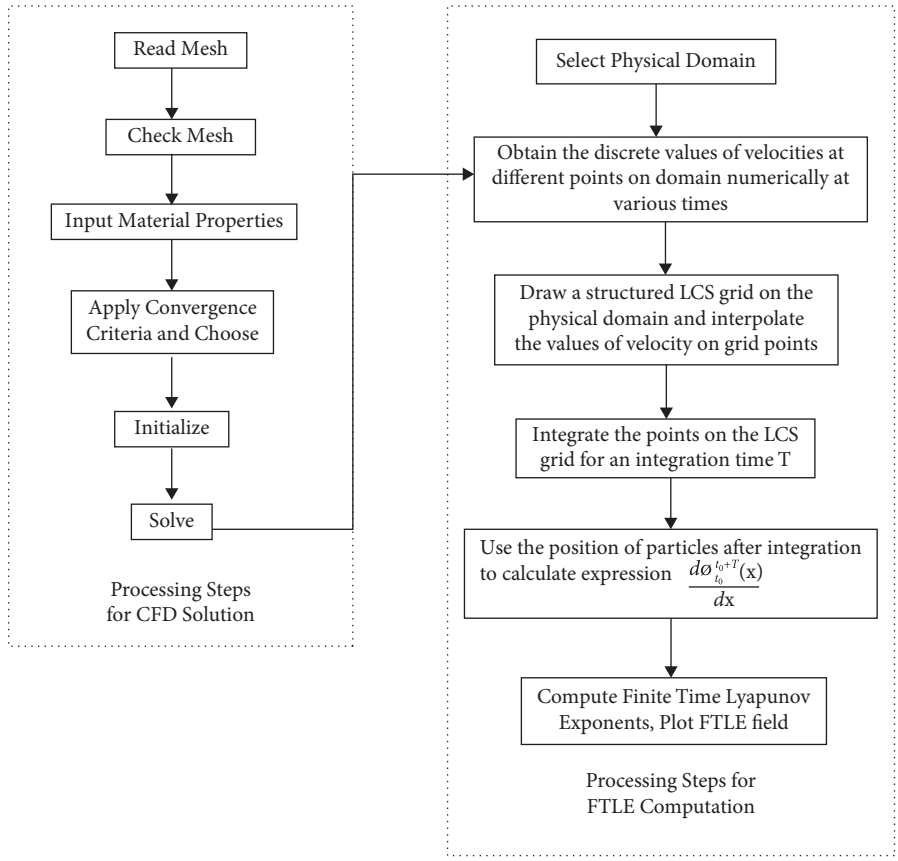

Figure 10: Flow map for LCS computation.

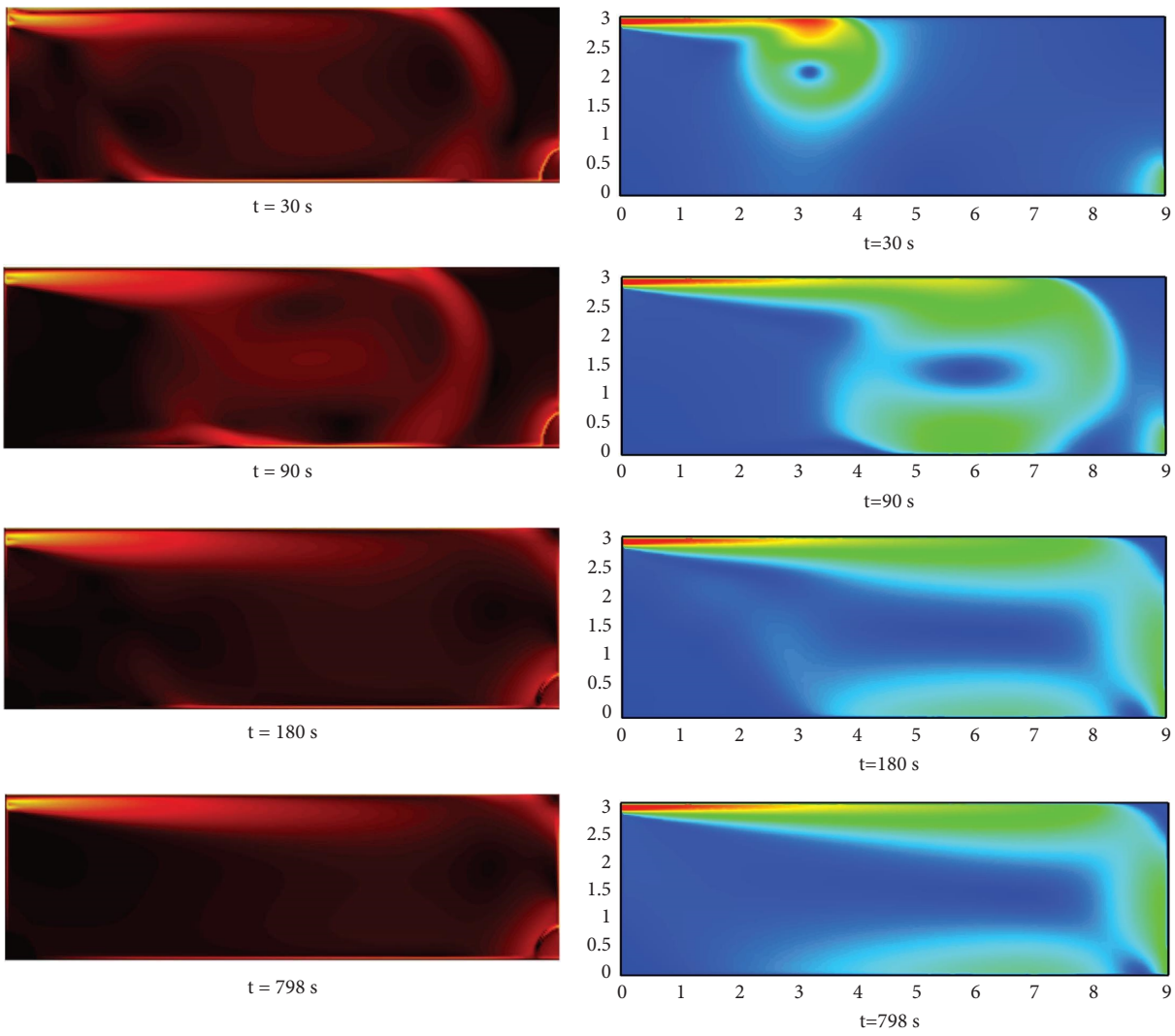

Figure 11: (a) LCS-2D-room ventilation, air inlet angle 0°. (b) Corresponding CFD results, air inlet angle 0°.

where $\overline{\delta x}(t_0)$ is aligned with the eigenvector associated with $\lambda_{\max}(\Delta)$. If we define

$$\sigma_{t_0}^{T}(\mathbf{x}) = \frac{\mathbf{1}}{|T|}\ln\sqrt{\boldsymbol{\lambda}_{\max}(\Delta)}, \tag{10}$$

then equation (9) can be rewritten as follows:

$$\max_{\delta \mathbf{x}(t_0)} \left\|\delta \mathbf{x}(t_0 + T)\right\| = e^{\sigma_{t_0}^{T}(\mathbf{x})|T|}\left\|\overline{\delta \mathbf{x}}(t_0)\right\|. \tag{11}$$

Equation (11) represents the finite time Lyapunov exponent at the point $x \in D$ at time t_0 with a finite integration time T.

To calculate the FTLE field, the initial information is available in the form of discrete set of data, which is often obtained from computational fluid dynamics or from direct measurements. An initial domain on which LCS are to be generated is selected. This domain consists of n number of particles which are arranged uniformly at time t. The trajectory of these particles is integrated for an integration time T. Due to this, the positions of these particles is changed and they assume at different positions. The new positions occupied by the particles as a result of evolving a trajectory at time $t + T$ is shown in Figure 9 [17].

The formula for the gradient of the flow map at an arbitrary point $x\,(i, j)$ using central differencing would be as follows:

$$\frac{d\varnothing_{t_0}^{t_0+T}(\mathbf{x})}{\mathrm{d}\mathbf{x}} = \begin{bmatrix} \dfrac{x_{i+1.j}^{(t+T)} - x_{i-1.j}^{(t+T)}}{x_{i+1.j}^{(t)} - x_{i-1.j}^{(t)}} & \dfrac{x_{i.j+1}^{(t+T)} - x_{i.j-1}^{(t+T)}}{y_{i.j+1}^{(t)} - y_{i.j-1}^{(t)}} \\ \dfrac{y_{i+1.j}^{(t+T)} - y_{i-1.j}^{(t+T)}}{x_{i+1.j}^{(t)} - x_{i-1.j}^{(t)}} & \dfrac{y_{i.j+1}^{(t+T)} - y_{i.j-1}^{(t+T)}}{y_{i.j+1}^{(t)} - y_{i.j-1}^{(t)}} \end{bmatrix}. \tag{12}$$

The value of the gradient is calculated on all the points on the grid and used in the FTLE equation (10) to the compute value of FTLE at each grid point. This data can be visualized by a color contour plot by using any visualizing data

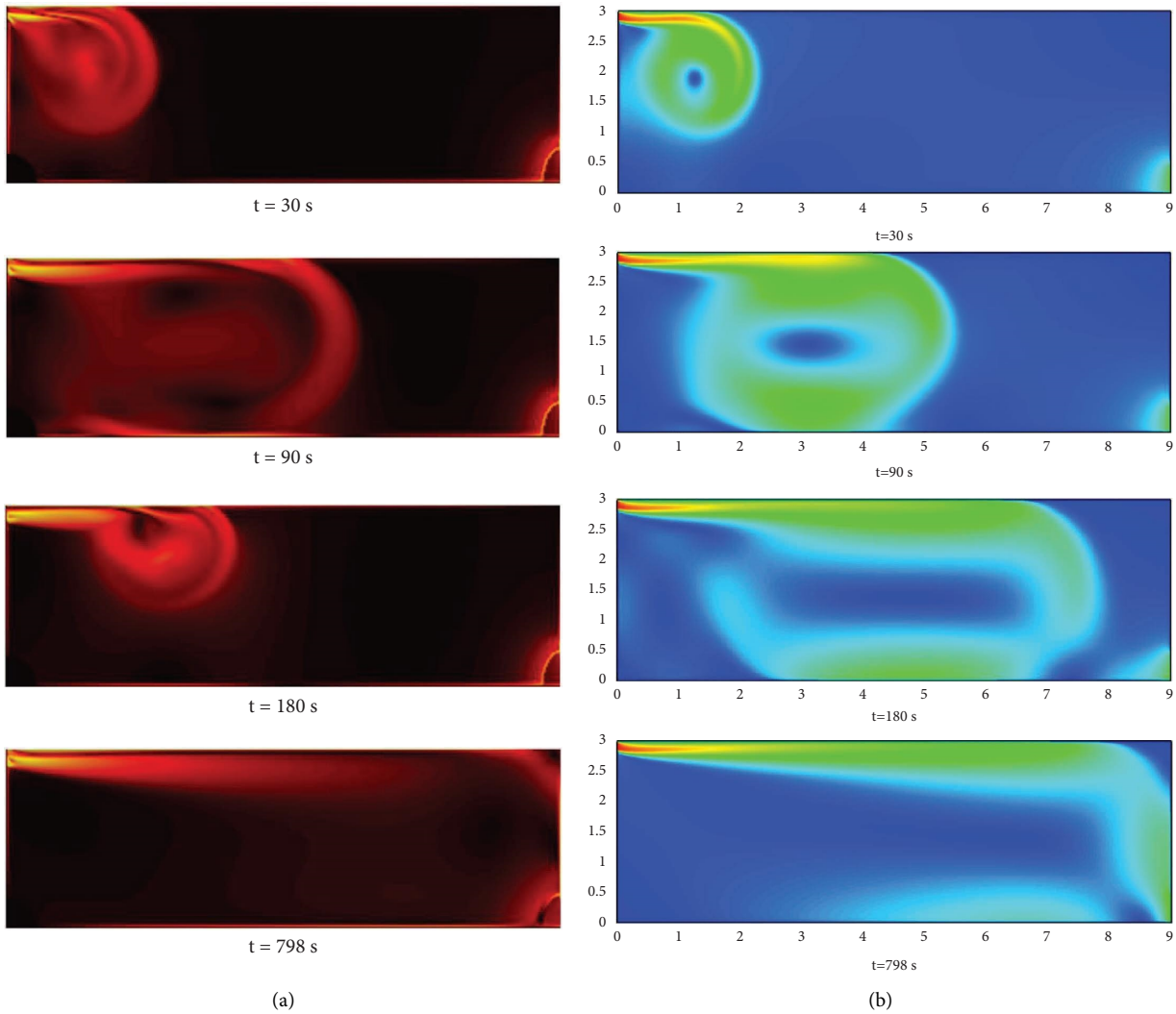

Figure 12: (a) LCS-2D-room ventilation, air inlet angle 15°. (b) Corresponding CFD results, air inlet angle 15°.

program or software. The flow map of FTLE computation is shown in Figure 10.

MATLAB code for Lagrangian coherent structures has been written and the discrete data obtained from the numerical simulation are plugged into the code. The values on the LCS grid are interpolated. The interpolated values are then used to integrate these grid points to generate stable or unstable manifolds for the finite time Lyapunov exponent field.

3.3.2. Lagrangian Coherent Structures on 2D Model Room. The main objective of the computational fluid dynamics analysis was to generate velocity data on grid points in the domain. The velocity data, hence, generated would be used for simulation of Lagrangian coherent structures, in which pattern of flow is delineated by virtual boundaries. This is the region where separation and transition occurs. The velocity data stored in the form of ASCII files are used to create both forward time finite time Lyapunov exponents and backward time finite time Lyapunov exponents. The manifolds, hence, created are analyzed to observe the structure of flow. Particles are seeded at different air inlet angle (0°, 15°, 22°, and 30°) and their trajectory corresponding to the Lagrangian coherent structures is observed at different time steps which are shown in Figures 11(a), 12(a), 13(a), and 14(a), respectively, and also shown corresponding CFD results in Figures 11(b), 12(b), 13(b), and 14(b), respectively, as a comparison purpose for two different numerical schemes.

4. Discussions

In this study, air flow analysis of 2D room was performed using CFD. The analysis was verified and validated with the results of Kayne and Agarwal [14]. After that, four CFD cases were studied based on air inlet angles (0°, 15°, 22°, and 30°) and air velocity data on these angles in 2D HVAC domain was acquired. This velocity data was further used in MATLAB code for FTLE computations in order to generate LCS boundary lines.

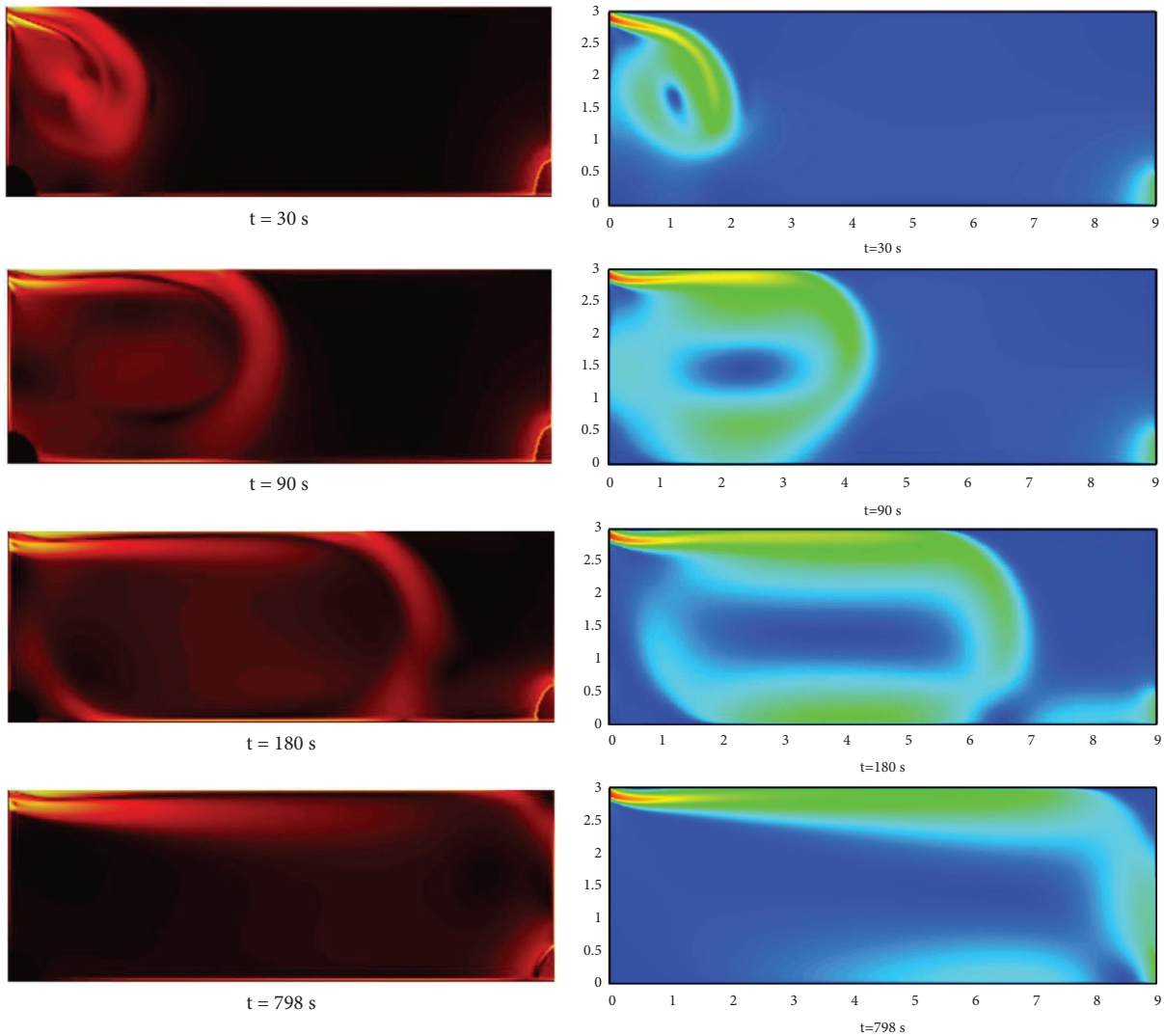

Figure 13: (a) LCS-2D-room ventilation, air inlet angle 22°. (b) Corresponding CFD results, air inlet angle 22°.

In the case with inlet angle 0° and 15°, it is observed that manifolds carry most of the fresh air out of the domain. There are regions inside the domain where flow remains stagnated. When the inlet angle of 22° is chosen, some fresh air reaches to the bottom center of the room. This case is considered to provide better ventilation then the previous one. Lastly, an angle of 30° is chosen for inlet air. In this case the fresh air first reaches the bottom center before being carried out of the domain by manifolds. The study shows that manifolds at 30° angles provide better ventilation of air. Using Lagrangian coherent structures to simulate ventilation problem can help in better designing ventilation systems.

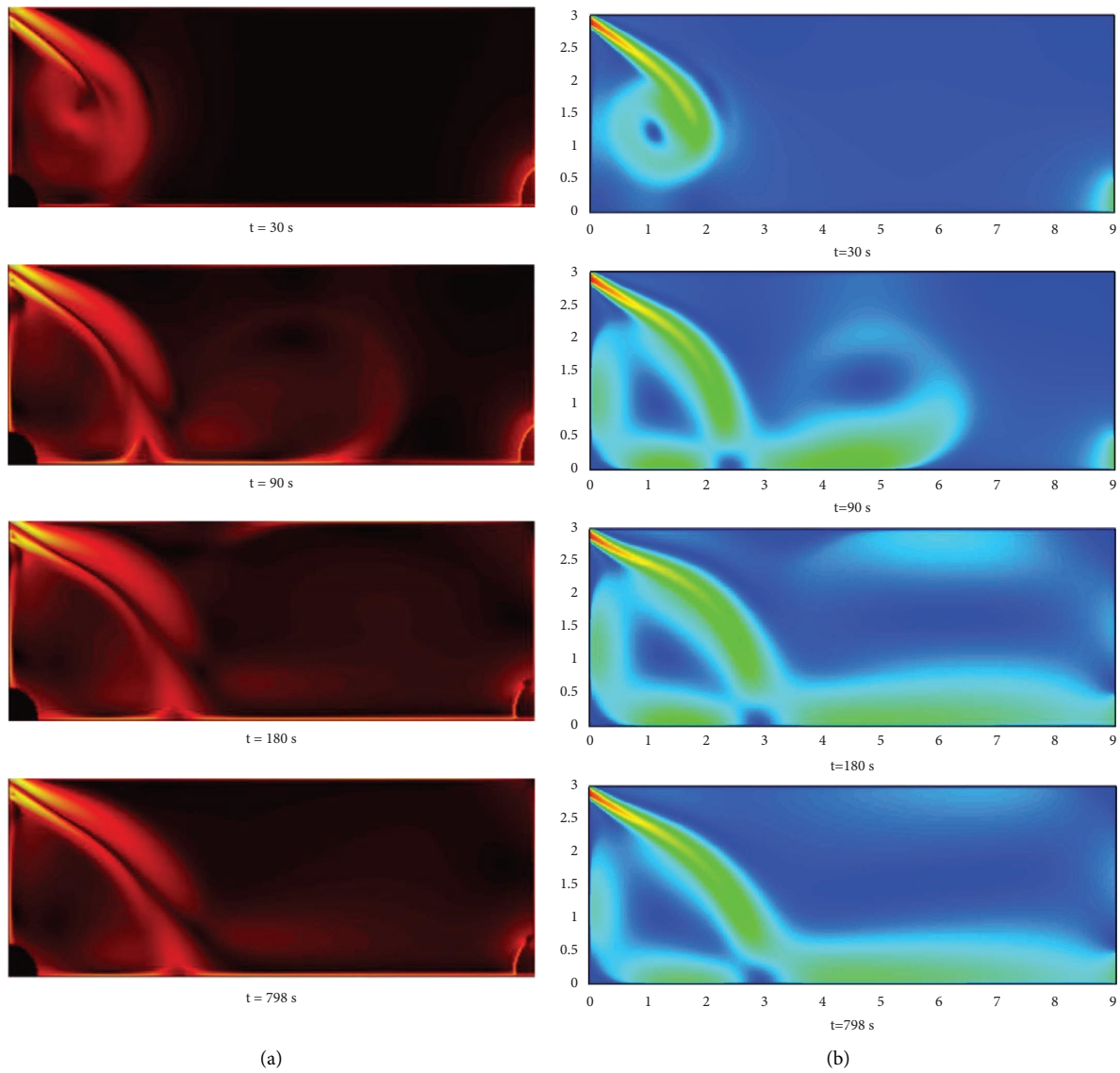

Figure 14: (a) LCS-2D-room ventilation, air inlet angle 30°. (b) Corresponding CFD results, air inlet angle 30°.

5. Conclusions

Lagrangian coherent structures was presented on 2D HVAC system. It is a method for identification of complex structures in fluid flow. It was shown how the use of this method provided additional information to the conventional methods used. The study shows presence of virtual walls inside the room. The presence of virtual walls has impact on the quality of ventilation in certain parts of the room. These walls are responsible for entraining particles and not letting fresh air in certain regions, while on the other hand, path for air flow created by manifolds in certain regions has helped in creating better ventilation. Using Lagrangian coherent structures to simulate ventilation problem can help in better designing ventilation systems. It can also help in modifying and optimizing the ventilation systems presently installed. Another approach for better design and optimization can be controlling the manifolds in order to have a desired pattern of air flow and, hence, ventilation. Lagrangian coherent structures have been applied to the applications such as oceanography, bio medical sciences, and several other fields. Lagrangian coherent structures can be used in dynamic simulation of heating ventilation and air conditioning systems. This would help identify flow barriers in a dynamic way and how they affect different parts of a building. A code to calculate three dimensional Lagrangian coherent structures is also possible. This would require an extra dimension in the modeling of FTLE. The results of a three dimensional code will show LCS as material surface rather than material lines as shown in the current two dimensional simulations.

Nomenclature

CFD: Computational fluid dynamics
FTLE: Finite time Lyapunov exponent
LCS: Lagrangian coherent structure

U/U_o: Normalized horizontal velocity
V/V_o: Normalized vertical velocity
Re: Reynolds number
$|T|$: Integration time length (s)
$\varnothing_{t_0}^{t_0+T}(\mathbf{x})$: Flow map describes the position information of the fluid particle at time $t = t_0 + T$
$\sigma_{t_0}^{T}(\mathbf{x})$: The finite time Lyapunov exponent defined as $\sigma_{t_0}^{T}(\mathbf{x}) = (1/|T|)\ln\sqrt{\lambda_{\max}(\Delta)}$.

Data Availability

The data used to support the findings of this study are available from the corresponding author upon request.

Additional Points

LCS Code Link. https://github.com/Dildar1/LCS-Code.git.

Conflicts of Interest

The authors declare that they have no conflicts of interest.

References

[1] J. W. Weathers, "Study of computational fluid dynamics applied to room air flow," Doctoral dissertation, Oklahoma State University, Stillwater, Oklahoma, 1992.
[2] G. Evola and V. Popov, "Computational analysis of wind driven natural ventilation in buildings," *Energy and Buildings*, vol. 38, no. 5, pp. 491–501, 2006.
[3] A. K. Elsadig, *Energy Efficiency in Commercial Buildings*, University of Strathclyde, Glasgow, Scotland, 2005.
[4] A. Kermani, "CFD modeling for ventilation system of a hospital room," 2015, https://www.comsol.com/paper/download/257311/kermani_paper.pdf.
[5] G. Haller and A. C. Poje, "Finite-time transport in aperiodic flows," *Physica D: Nonlinear Phenomena*, vol. 119, no. 3-4, pp. 352–380, 1998.
[6] V. L. Rom-Kedar, A. Leonard, and S. Wiggins, "An analytical study of transport, mixing and chaos in an unsteady vortical flow," *Journal of Fluid Mechanics*, vol. 214, no. -1, pp. 347–394, 1990.
[7] M. F. Detaranto, *CFD Analysis of Airflow Patterns and Heat Transfer in Small, Medium, and Large Structures*, Doctoral dissertation, Virginia Tech, Blacksburg, VA, USA, 2014.
[8] G. Haller and G. Yuan, "Lagrangian coherent structures and mixing in two-dimensional turbulence," *Physica D: Nonlinear Phenomena*, vol. 147, no. 3-4, pp. 352–370, 2000.
[9] S. C. Shadden, F. Lekien, and J. E. Marsden, "Definition and properties of Lagrangian coherent structures from finite-time Lyapunov exponents in two-dimensional aperiodic flows," *Physica D: Nonlinear Phenomena*, vol. 212, no. 3-4, pp. 271–304, 2005.
[10] F. Lekien, C. Coulliette, A. J. Mariano et al., "Pollution release tied to invariant manifolds: a case study for the coast of Florida," *Physica D: Nonlinear Phenomena*, vol. 210, no. 1-2, pp. 1–20, 2005.
[11] A. B. Olcay, "Investigation of a wake formation for flow over a cylinder using Lagrangian coherent structures," *Progress in Computational Fluid Dynamics, an International Journal*, vol. 16, no. 2, pp. 126–130, 2016.
[12] S. C. Shadden, M. Astorino, and J. F. Gerbeau, "Computational analysis of an aortic valve jet with Lagrangian coherent structures," *Chaos: An Interdisciplinary Journal of Nonlinear Science*, vol. 20, no. 1, Article ID 017512, 2010.
[13] S. C. Shadden, *A Dynamical Systems Approach to Unsteady Systems*, California Institute of Technology, Pasadena, CA, USA, 2006.
[14] A. Kayne and R. Agarwal, "Computational Fluid dynamics modeling of mixed convection flows in building enclosures," *American Society of Mechanical Engineers*, vol. 55515, Article ID V001T01A004, 2013.
[15] J. M. Ottino and J. M. Ottino, *The Kinematics of Mixing: Stretching, Chaos, and Transport*, Cambridge University Press, Cambridge, UK, 1989.
[16] G. Haller, "Lagrangian coherent structures from approximate velocity data," *The Physics of Fluids*, vol. 14, no. 6, pp. 1851–1861, 2002.
[17] G. Haller, "Distinguished material surfaces and coherent structures in three-dimensional fluid flows," *Physica D: Nonlinear Phenomena*, vol. 149, no. 4, pp. 248–277, 2001.